JOURNAL OF MATERIALS SCIENCE **36** (2001) 3323–3332

Hydroxyapatite-316L fibre composites prepared by vibration assisted slip casting

X. MIAO
Graduate School of Biomedical Engineering, University of New South Wales, Sydney, NSW 2052, Australia

A. J. RUYS
Department of Mechanical & Mechatronic Engineering, University of Sydney, Sydney, NSW 2006, Australia

B. K. MILTHORPE*
Graduate School of Biomedical Engineering, University of New South Wales, Sydney, NSW 2052, Australia

To prepare hydroxyapatite (HA, or HAp)-stainless steel 316L fibre composites with up to 30 vol% 316L fibres (~1 mm long and 50 μm in diameter), slip casting assisted by vibration (frequency: ~55 Hz; amplitude: ~5 mm) was carried out, followed by both cold isostatic pressing (CIPing) and hot isostatic pressing (HIPing). With the addition of around 0.5 wt% sodium carboxymethylcellulose (Na-cmc), solids loadings up to 44 vol% were obtained in calcined HA powder-derived slips, which were castable only under the vibration. The slips were concentrated and viscous so that the preferential sedimentation of the dense and large 316L fibres could be avoided. Subsequent CIPing was able to increase the relative density of the cast and dried green compacts from 46% after casting to 60% after CIPing. With the dense and uniform green compacts of the HA-316L mixtures, final HIPing at 950 °C resulted in HA-316L fibre composites of 99% relative density. The HA-316L fibre composites had improved fracture toughness of 3.6 ± 0.3 MPa.m$^{0.5}$, due to the bridging effect of the ductile 316L fibres. However, the mechanical strength of the composites was limited by the presence of residual thermal stresses and circumferential microcracks. The HA-316L fibre composites were biocompatible and exhibited favourable bone-bonding characteristics.

1. Introduction

Hydroxyapatite (HA) ceramic materials and coatings have been reported to exhibit excellent characteristics of direct chemical and mechanical bonding with natural bones when compared to inert ceramic and metal materials [1–3]. Thus, medical grade HA granules and preforms have been used for bone grafting and augmentation in maxillofacial surgery and in orthopaedics [4] as space filling materials. However, HA ceramics have insufficiently good mechanical properties for major load bearing applications.

In addition, the tensile strength of the HA to bone bond for solid HA and coatings has been found to be low, of the order of 0.5 to 1.5 MPa [5, 6]. For highly polished surfaces [5] the low tensile strength appeared to be due to poor bonding to HA at early times (33 days) unless partial degradation of the surfaces provided some mechanical interlock. At later time periods the failure due to a more severe degradation of the HA along the grain boundaries tended to reduce the measured interface strength. Gross *et al*. [7] have shown that increased surface roughness correlates with increased tensile strength of the bone-HA interface.

For HA to be useful in load bearing applications as a replacement graft material (as opposed to a tissue engineering support) it must remain essentially intact, have a strength and toughness close to that of bone. It would also be an advantage to have tensile and shear strengths of the bone-HA interface that are close to that of bone. However engineering techniques that produce interfaces that are not normal to the direction of major tensile loads or parallel to shear loads can reduce the dependence on tensile strength. The generation of a useable HA material, therefore, requires first satisfying the mechanical strength and toughness criteria.

One way to improve the mechanical properties of HA ceramics is to develop HA matrix composites [8]. It is known that whiskers and fibres have the most effective toughening effect [9], but whiskers are not recommended due to their potential carcinogenicity. Short fibres can be advantageous compared with long continuous fibres since short fibres can act as particles when

* Author to whom all correspondence should be addressed.

mixed with matrix powders during forming. Short stainless steel 316L fibre reinforced HA composites are considered as candidate materials. This is because stainless steel 316L is a biocompatible material with thermal expansion coefficients close to those of HA ceramics [10]. The 316L fibres are also expected to have significant toughening effects on the HA-based composites [11].

Compared with extrusion and injection moulding, dry pressing and slip casting are relatively simple bulk forming methods. Uniaxial dry pressing however limits the formed shapes to disks or bars. Slip casting (including drain slip casting and solid slip casting) is commonly used for preparing pure HA ceramics. For example, Simoes *et al*. [12] prepared HA bodies with differential porosity by slip casting. Lelievre *et al*. [13] also obtained HA ceramics by casting optimised suspensions. However, conventional slip casting is not quite suitable for preparing 316L fibre-reinforced composites due to the following problems encountered. Wet mixing is a common practice to achieve phase homogeneity, but the 316L fibres are so dense that preferential sedimentation of the fibres occurs. Ball milling or attrition milling due to the presence of milling medium also causes entanglement of the ductile 316L fibres. Solid slip casting requires a slip of certain concentration for the castability of the slip, but the concentration is normally not high enough to prevent preferential sedimentation of the fibres. Apart from the problems associated with slip casting, the HA-316L fibre composites cannot be sintered in air due to oxidation of the fibres. The composites cannot be densified in a protective atmosphere either due to the shrinkage constraint of the fibre network. The decomposition of the HA component at high sintering temperatures is another common problem.

We have made efforts to overcome the above difficulties in order to prepare HA-316L composites. To homogenise the short 316L fibres, we have tried vibration assisted and medium-free mixing of the dry HA-316L mixtures and the concentrated slips of the mixtures. To form the green bodies of the composites by casting, we have taken advantage of the thixotropic behaviour of the concentrated HA based slurries dispersed with a polyelectrolyte. Thixotropic suspensions are normally flocculated when there is no mechanical interference acting on them, but are fluids (castable) under vibration or shearing. Thus, with the help of mechanical vibration in the solid slip casting, a compromise can be made between the castability of the concentrated slips and the prevention of the preferential sedimentation of the fibres. Finally, to achieve full densification of the HA-316L composites without the decomposition of the HA component, both cold and hot isostatic pressing processes have been jointly adopted. Both CIPing and HIPing have the capability of forming complex shapes. Compared with hot pressing, HIPing can also achieve higher compaction pressures thus the composites can be densified at lower temperatures. The aim of this paper is to report on the preparation of the HA-316L fibre composites based on vibration assisted solid slip casting. The microstructural, mechanical, and initial biological characterisations of the HA-316L fibre composites are also presented.

2. Experimental procedures

The as-supplied HA powder (E. Merck, D-6100 Darmstadt, Germany) consisted of micron scale sized agglomerates, which in turn consisted of nanometre sized primary particles and open pores between the primary particles (Fig. 1). To modify the as supplied HA powder, calcination at 900 °C for 1 hour in air was carried out. The calcined HA powder consisted of agglomerates of submicron sized primary particles partially sintered together (Fig. 2). Short stainless steel 316L fibres about 1 mm long were obtained by chopping continuous 316L fibres of 50 μm in diameter (Knight Precision Wires, UK) followed by ultrasonic cleaning with boiling water, acetone, and ethanol (Fig. 3). Sodium carboxymethylcellulose (Na-cmc; Daicel 1130) was dissolved in de-ionised water by magnetic stirring to prepare Na-cmc sols of different contents (0.1–3.00 wt%).

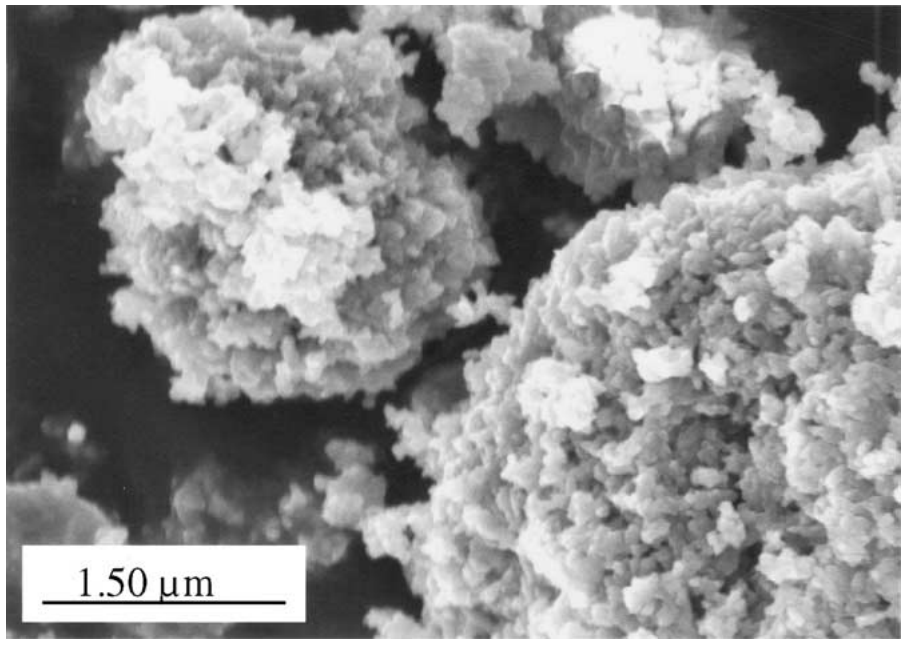

Figure 1 SEM micrograph showing the morphology of the as supplied hydroxyapatite (HA) powder.

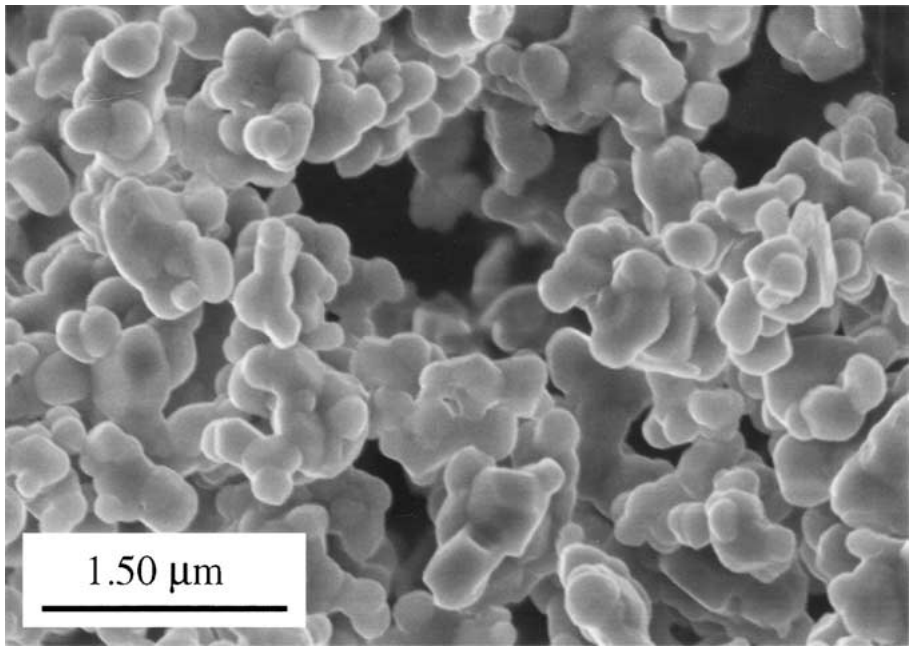

Figure 2 SEM micrograph showing the morphology of the HA powder after calcination at 900 °C for 1 hour.

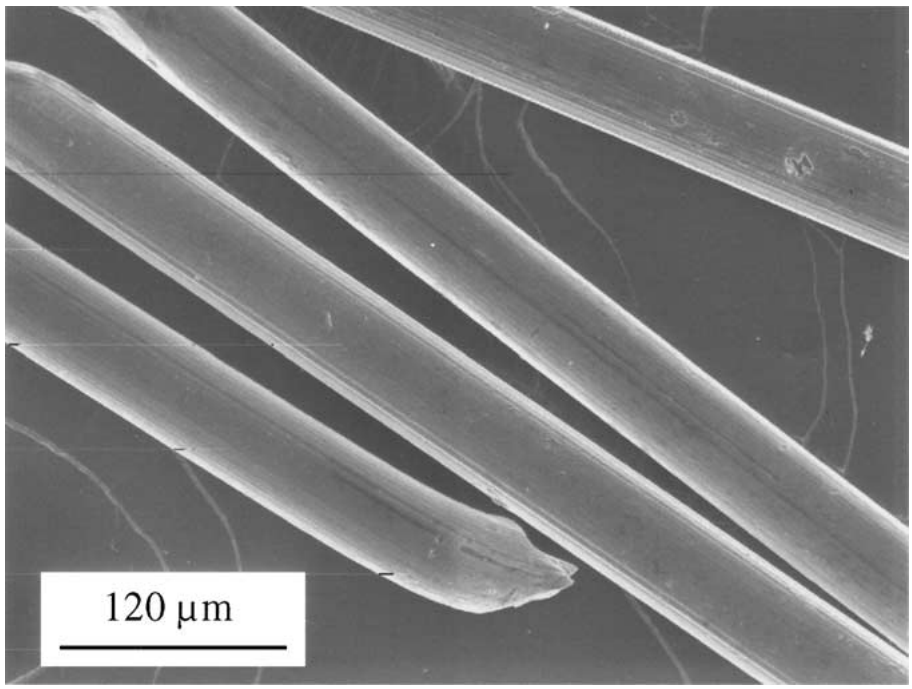

Figure 3 SEM micrograph showing the morphology of the chopped stainless steel 316L fibres.

The Na-cmc sols acted as a deflocculant, a binder, and a thixotropy inducer [14, 15].

To obtain the "optimal solids loading" of a calcined HA based slip, a Na-cmc sol of a known concentration was incrementally added into a certain amount of the calcined HA powder. After being homogenised by the vibration (frequency: ∼55 Hz; amplitude: ∼5 mm), the slip finally reached a certain viscosity (optimal rheology), which rendered the slip just castable under vibration. The optimal solids loading (vol%) of the slip and the corresponding optimal Na-cmc content (wt%) were then calculated from the amounts of the used HA powder and the added Na-cmc sol. To obtain the optimal solids loading of a HA-316L mixture slip, the HA-316L mixture was mixed with the Na-cmc sol of the concentration that was optimised previously for the corresponding pure HA slips. Other procedures for making the slips castable just under vibration and methods of calculating the optimal solids loading of the HA-316L mixtures were similar to those described for the pure HA slips. To further study the thixotropic behaviour of the calcined HA based slips, the calcined HA powder was mixed with a 1 wt% Na-cmc sol until certain solids loadings (25–37.5 vol%) were reached. The viscosity of the slips was then measured at different shear rates (50 s-1 and 85 s-1). The viscosity of the slips with various solids loadings was measured using a programmable rheometer (Brookfield, Model DV - III, USA).

When the optimised slips of the HA-316L mixtures were made castable under vibration, they were then formed into cylindrical green compacts by slip casting with porous plastic moulds attached to a vibrating stage (frequency: ~55 Hz; amplitude: ~5 mm). Immediately after being removed from the vibration, the cast slips became gelled or flocculated, thus preventing the preferential sedimentation of the 316L fibres. The cast cylinders were then dried in an oven at 110 °C for 12 hours. After drying, some cast cylinders were further compacted by cold isostatic pressing at 160 MPa. The density of the green compacts was determined by measuring the weight and volume of the green compacts. Three measurements were done to obtain an average density. Some CIPed green compacts based on the calcined HA powder were evacuated and sealed in glass capsules filled with BN powder as a diffusion barrier. The sealed samples were then hot isostatically pressed (HIPed or Hipped) at 950 °C, under 124 MPa, and for 1.5 hours using a AIP 6-30H machine (American Isostatic Pressing Inc., USA). A dense HA cylinder was also prepared by sintering a CIPed HA cylinder at 1250 °C for 2 hours in air. The density of the sintered and the HIPed samples was measured based on the Archimedes' principle using distilled water as medium on a precision electric balance.

Phase analysis on the polished surfaces of the HIPed samples was conducted by x-ray diffraction (XRD) using a Siemens D5000 diffractometer. The working conditions of the diffractometer included an electric voltage of 30 kV and an electron beam current of 30 μA. The morphology of the staring HA powders and the 316L fibres was observed by scanning electron microscopy (SEM) on a Hitachi 4500 – II machine. The distribution of the 316L fibres in the HA matrices of the HIPed samples was also examined on polished surfaces. The fracture surfaces of the composite samples were also examined by SEM. For the SEM observations, all the samples were coated with an electrically conductive carbon film.

Some sintered and HIPed cylinders were machined into bar specimens with dimensions of 3 to 4 by 3 to 4 by about 40 (mm) for bending strength measurements and 3 to 4 by 6 to 8 by about 40 (mm) for fracture toughness measurements. For the fracture toughness measurements, each of the bar specimens was further machined to produce a notch, with the notch width being about 300 μm and the ratio of the notch depth to the specimen thickness being about 0.5. The bending strength (σ_{3pt}) and the fracture toughness (K_{1c}) were measured in a three-point bending set-up on an Instron 4302 machine at the crosshead speed of 0.5 mm/min. The bending strength and the fracture toughness values were calculated using the formulae listed by Richerson [16]. In addition, the interaction of indentation cracks with the 316L fibres was studied on a hardness testing machine (M-400-HI, Leco).

The *in vitro* biocompatibility of the HA-316L fibre composites was evaluated according to ASTM Standard F 813–83 (Standard Practice for Direct Contact Cell Culture Evaluation of Materials for Medical Devices). In this evaluation, each polished and sterilised disk sample was placed on a confluent L-929 cell monolayer in a Petri dish. After incubation at 37 °C, an optical microscope was used to assess the degree of cytotoxicity of the samples. In vivo evaluation especially bone bonding performance was also carried out with the materials of HA ceramics, HA-25 vol% 316L fibre composite, and silicon nitride (with a high porosity and prepared by reaction sintering). The latter was used as a reference due to its bioinertness. For the measurement of bone-material bonding strength, polished and sterilised bar samples ($3 \times 3 \times 12$ mm^3) were implanted into the 4 tibiae of two sheep. Each tibia was implanted with 6 implants and 1 drilled hole as a control, spaced at 2 cm apart. After 4 weeks the sheep were sacrificed and the implants were removed by sectioning 1 cm above and below each implant. Each section of tibia was then fixed with a 10% neutral phosphate-buffered formalin solution. With a fine diamond grit impregnated band saw (EXAKT), bar specimens each containing two bone segments with one implant segment in between were cut from the fixed bone sections each with an implant. Finally the bone-material bonding strength was measured on a Instron 4302 (Instron, UK) using a cantilever bending set up at the crosshead speed of 0.5 mm/min. The bone/implant interfacial bonding strength, σ, was calculated using the following formula:

$$\sigma = \frac{6PL}{bd^2} \tag{1}$$

where P is the maximum load in a load-extension curve, L is the distance from a selected bone/implant interface to the round edge of a loading knife, b is the width (perpendicular to the loading direction) of the uniform cross section of the bone/implant/bone specimen, d is the thickness (parallel to the loading direction) of the cross section.

3. Results and discussion

Fig. 4 shows the optimal solids loading as a function of the optimal Na-cmc content for the calcined HA powder. Any point on or close to the curve represents a set

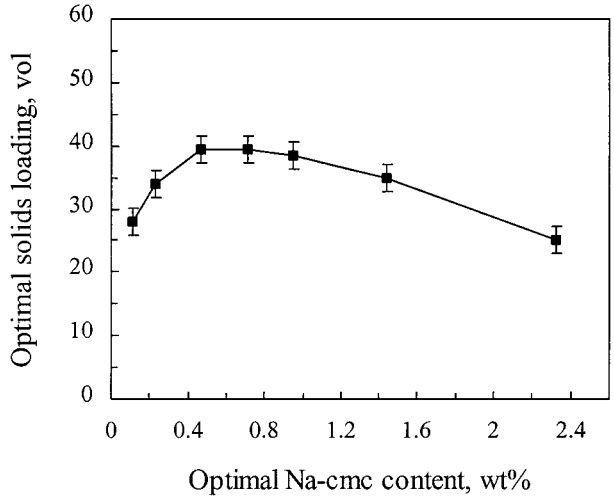

Figure 4 Optimal solids loading versus optimal Na-cmc content for the slips prepared from the calcined HA powder and the Na-cmc sols of different concentrations (Na-cmc: sodium carboxymethylcellulose).

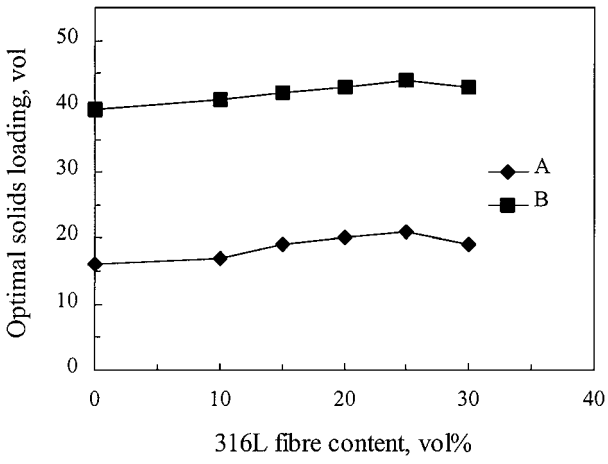

Figure 5 Optimal solids loading versus 316L fibre content for the slips prepared from the HA-316L fibre mixtures and the 1 wt% Na-cmc sol. A: as-supplied HA powder based; B: calcined HA powder based.

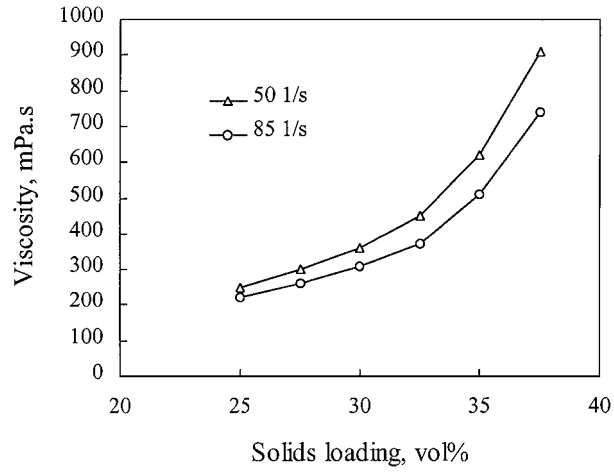

Figure 6 Viscosity versus solids loading for the slips prepared from the calcined HA powder and the 1 wt% Na-cmc sol.

of solids loading and Na-cmc content values that make a slip castable (liquid-like) under vibration but flocculated (solid-like) when in standstill. A slip cannot be cast even under vibration, when it has a set of solids loading and Na-cmc content values located in the region above the curve. The maximum optimal solids loading appeared within a range but around the Na-cmc content of 0.5 wt%. Thus, in that range of Na-cmc content, the HA particle agglomerates were relatively well dispersed in the slips, which were flowable under vibration. The fact that the maximum optimal solids loading could be obtained in a wide range of the Na-cmc content made processing control convenient.

When the 1 wt% Na-cmc sol was added into the as supplied and the calcined HA powders mixed with the 316L fibres, optimised slips castable just under vibration were obtained. Fig. 5 shows that the optimal solids loading slightly increased with the 316L fibre content. This means that for a unit volume of the HA-316L fibre mixtures, higher fibre content required less amount of Na-cmc sol in order to reach the same flowability. This result can be explained by the slight increase of the surface area per unit volume of the HA-316L fibre mixtures. Since the 316L fibres were much larger in size ($\sim$1 mm long and 50 μm in diameter) than the HA powders, the addition of the fibres decreased the surface area per unit volume of the mixtures. Thus the lower surface area per unit volume required less amount of Na-cmc sol to wet the particle surfaces and form a polymer/ water film. Only when the sol content sufficiently exceeded the volume of pores among the agglomerates to separate the agglomerates for a certain distance could any reasonable fluidity be expected. However, the solids loading did not increase significantly with the increasing fibre content. The large amount of the fibres in the slips may adversely decrease the flowability of the slips.

Fig. 5 also shows that the as supplied HA powder resulted in lower optimal solids loading than the calcined HA powder. In fact, our experiments indicated that the Na-cmc additive was not effective in dispersing the as supplied HA powder; Na-cmc addition in the range of 0.2–4 wt% (solid basis) all resulted in optimal solids loading only between 16–18 vol%. This may be due to the nanometre scale particle size and the complex nature of the as supplied HA particle surfaces. It is a common fact that high specific surface area of particles limits the maximum solids loading attainable [17]. Lelievre *et al.* [13] also reported that the electric charges developed on the surface of the HA particles in the presence of a dispersant were changed with calcination temperature.

Fig. 6 shows the viscosity of the slips derived from the calcined HA powder and the 1 wt% Na-cmc sol, which was dependent on the solids loading and the shear rate. It can be seen that with the increase of solids loading, there was an increase in the difference in viscosity measured at shear rates of 50 s^{-1} and 85 s^{-1}, respectively; slips of higher solids loading were more thixotropic. For a given viscosity level required for the solid slip casting, thixotropic slips under higher shear rates could be castable at higher solids loadings. Compared with normal solid slip casting, the solid slip casting under vibration resulted in castable slips of higher solids loadings due to the higher shear rates generated. If the solids loading of a slip was too high, the vibration could not make the slip castable. If a slip were too dilute, the component particles of different size and density would cause preferential sedimentation.

Fig. 7 shows the effect of the 316L fibre content on the relative density of the HA-316L fibre green compacts prepared by casting and casting-CIPing, respectively. Comparing the curve B in Fig. 7 with the curve B in Fig. 5, one can see that there is not much difference in value between the optimal solids loading and the relevant density for the calcined HA powder derived mixtures. However, comparing the curve A in Fig. 7 with the curve A in Fig. 5, one can see the much higher relative density than the optimal solids loading for the as supplied HA powder derived mixtures. This suggests that for the calcined HA powder derived mixtures there was not much drying shrinkage from the wet slips to the dry compacts; whereas for the as supplied HA powder derived mixtures the drying shrinkage from the wet slips to the dry compacts was relatively noticeable.

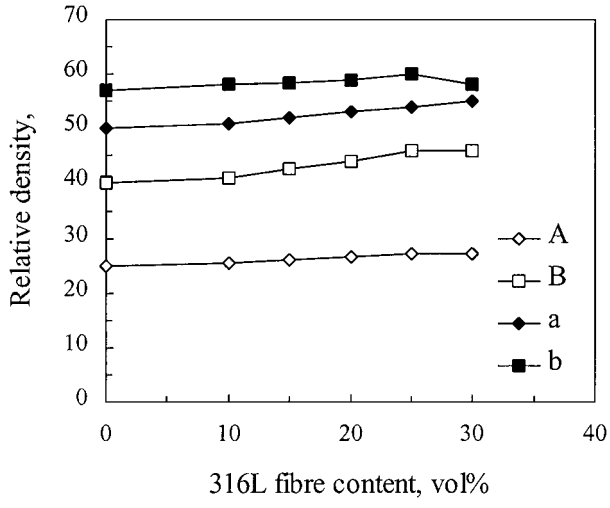

Figure 7 Relative density of green compacts versus 316L fibre content. A: dry cast compacts from the as supplied HA powder; B: dry cast compacts from the calcined HA powder; a: the same as A plus CIPing at 160 MPa; b: the same as B plus CIPing at 160 MPa.

The relationship between the optimal solids loading and the relative density can be seen more clearly with the following consideration. The solids loading (S.L.) of a slip can be derived from the real volume of the solids (Vs-real), the volume of the pores inside the solids (Vp-open; assuming the solids (particle agglomerates) contain only open pores), and the volume of the liquid between the solids (Vl-out), thus

$$\text{S.L.} = \frac{V_{\text{S-real}}}{V_{\text{S-real}} + V_{\text{p-open}} + V_{\text{l-out}}} \quad (2)$$

When the Vl-out reaches a minimum, i.e., Min {Vl-out}, the S.L. will reach a maximum, i.e., optimal solids loading Opt {S.L.}. On the other hand, one can derive the relative density (R.D.) of the green compact formed from the same slip, thus

$$\text{R.D.} = \frac{V_{\text{S-real}}}{V_{\text{S-real}} + V_{\text{p-open}} + V_{\text{p-out}}} \quad (3)$$

where Vp-out is the volume of the pores between the contacting agglomerates. When Vp-out $\approx$ Vl-out, i.e., there is not much volume shrinkage from the wet slip to the dry compact, Opt {S.L.} $\approx$ R.D., i.e., the optimal solids loading is close to the relative density.

Fig. 7 also shows the effect of the CIPing on the relative density of the cast green compacts. The as supplied HA powder derived cast compacts resulted in higher increase in the relative density than the calcined HA powder derived compacts. This was because the as supplied HA powder derived cast bodies contained higher porosity than the calcined HA powder derived cast bodies. Higher porosity resulted in low strength of a powder compact, which was more amenable to compaction [18]. The increase in relative density of the CIPed bodies resulted from the deformation and breakdown of the particle agglomerates and thus the removal of parts of the interagglomerate pores and intraagglomerate pores. Consequently, the strength of the CIPed green compacts was so high that rigorous handling, cutting, or drilling was possible. Fig. 7 also shows that the as supplied HA powder resulted in lower green density than the calcined HA powder. The as supplied HA powder derived cast bodies also had a large drying shrinkage and drying cracks were observed in the cast bodies. Thus, the calcined HA powder was better than the as supplied HA powder in terms of the control of the green compact size and shape.

The combination of vibration casting and CIPing was advantageous over the vibration casting or CIPing alone. When only CIPing was used, large reduction in volume of the loose powders was needed to get high density, which tended to result in density gradient and preferential fibre alignment. CIPing after the vibration casting could increase the density without affecting the orientation too much because of the much lower volume reduction. If vibration casting was used alone, high green density was difficult to achieve. This was because the current powders were fine in particle size and far from spherical in particle shape, and the Na-cmc additive resulted in slightly flocculation at low solids loading but pronounced flocculation at high solids loading. Thus the optimal solids loadings of the slips castable under the vibration were still not very high. Fortunately, the flocculation of the slurries induced the thixotropic behaviour [19, 20], which allowed the HA powders to hold the fibres in their positions against the preferential segregation and made the relatively concentrated slips castable under the vibration. The fulfilment of the homogenisation of the fibres was unavoidably at the expense of the green density of the cast samples, which was easily compensated for by the CIPing process.

The CIPed green compacts of the HA-316L fibre mixtures were densified by hot isostatic pressing (HIPing) to near 99% theoretical density assuming the theoretical density of HA being 3160 kg/m^3 and 316L 7950 kg/m^3. The high density was also confirmed by examining the fracture surface of the HA matrix under SEM (Fig. 8). The observed cavities in Fig. 8 were due to the pullout of grains (intergranular fracture) rather than the presence of pores. The HA component did not suffer from any decomposition after HIPing, as was confirmed by XRD (Fig. 9). Fig. 10 shows the different cross-section sizes and shapes of the 316L fibres, which were formed by the polished surface sectioning the 316L fibres in different directions. Thus a relatively random orientation of the 316L fibres was achieved. Fig. 10 also shows some defects on the polished surface; some of the defects obviously resulted from the grinding and polishing process used for the sample preparation. Fig. 11 shows a magnified area from Fig. 10 where microcracks around the 316L fibres were found.

Table I shows the mechanical property data of pure HA ceramics and HA-316L fibre composites. HIPed HA samples had improved mechanical properties compared with sintered HA ceramics. The fracture toughness of the composites was about 3 times of that of the pure HA ceramics, whereas the mechanical strength of the composites was not improved. Table I also lists the

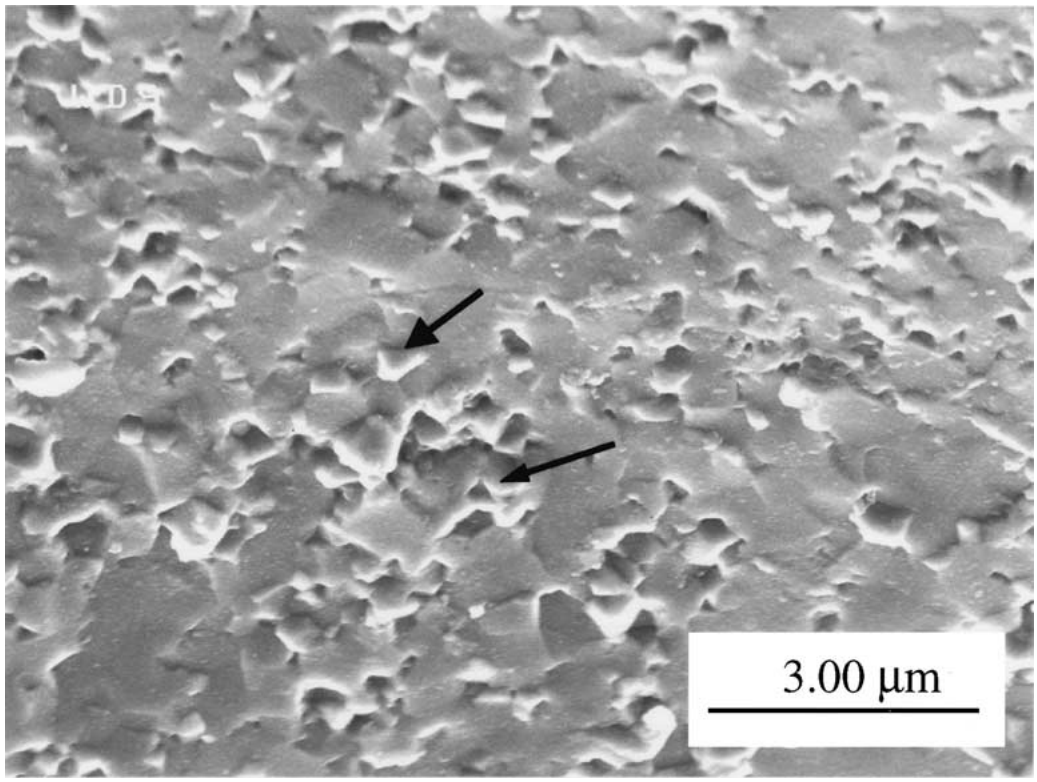

Figure 8 SEM micrograph showing the fracture surface of the HA matrix (from calcined HA powder) of the HA-25 vol% 316L fibre composite HIPed at 950 °C and 124 MPa.

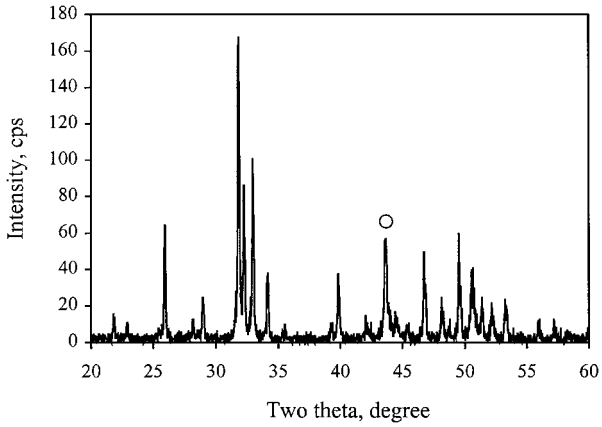

Figure 9 XRD diagram showing the pure HA phase (all unmarked peaks) and the 316L phase (marked with a circle).

calculated flaw size, which can be estimated according to the following formula:

$$K_{1c} = Y\sigma_{3pt}\, c^{0.5} \tag{4}$$

where K_{1c} is fracture toughness, σ_{3pt} is fracture strength, c is the half-length of a crack (or flaw), and Y is a dimensionless term determined by the crack configuration and taken as 1.26 [11] for a rough estimate. Thus, one can see that the improvement of the mechanical properties of the composites was limited by the large flaw size. This size was near the length of the fibres used. Thus the observed circumferential microcracks may be a source of the flaws. It is postulated that finer fibres if used would reduce the size of flaws and thus improve the mechanical properties.

TABLE I Mechanical properties of the HAp-316L composites

Material	σ_{3pt} (MPa)	K_{1c} (MPa · m$^{1/2}$)	$2c$ ($\times 10^{-6}$ m)
HAp sintered	63 ± 5	0.8 ± 0.1	204
HAp Hipped	96 ± 4	1.0 ± 0.2	137
HAp + 15 vol.% 316L fibres (Hipped)	92 ± 6	2.8 ± 0.3	1170
HAp + 25 vol.% 316L fibres (Hipped)	113 ± 9	3.6 ± 0.3	1281

Fig. 12 shows the three point bending curve of compression load versus deflection. The shape of the curve suggests a "pseudo-plasticity" of the composites, resulting from the reinforcing fibres. Fig. 13 shows the protruding ends of the fibres on the fracture surface. This could be the result of deflection of propagating cracks by the 316L fibres. Indentation on a polished sample at 1 kg load confirmed this crack deflection mechanism. Fig. 14 shows the existence of fibre fracture, which indicates the operation of fibre bridging mechanism. The "pseudo-plasticity" of the composites may be due to the fracture of the ductile metal fibres. For fibre bridging mechanism, the fibres need to be strongly bonded with the matrix, and a random orientation of the fibres is also important.

The direct contact assay indicated that the HA-316L fibre composites were biocompatible *in vitro*; no cytotoxicity was found. With regard to the in vivo assessment based on the four week implantation, it was found that the bone-material bonding strengths for HA, HA-316L, Si_3N_4, and Hole (newly formed bone) were 2.4 ± 0.4, 2.2 ± 0.3, 1.0 ± 0.2, and 5.5 ± 0.8 MPa, respectively. The HA ceramics and the HA-316L composites had superior bonding strength to the reaction bonded Si_3N_4 ceramics. This can be explained by the

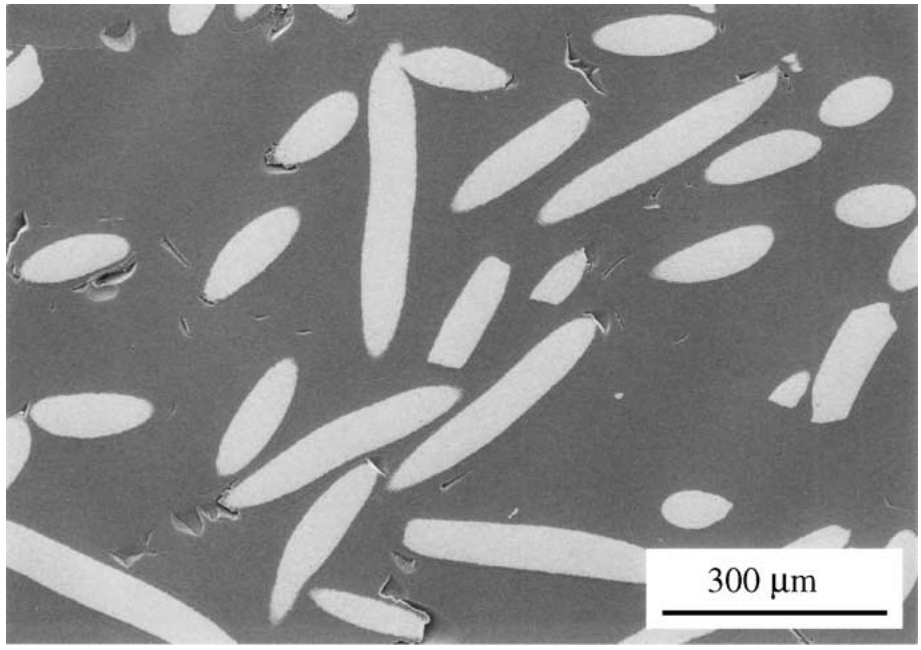

Figure 10 SEM micrograph showing the relatively random distribution of the 316L fibres in the HA-25 vol% 316L fibre composite HIPed at 950 °C and 124 MPa.

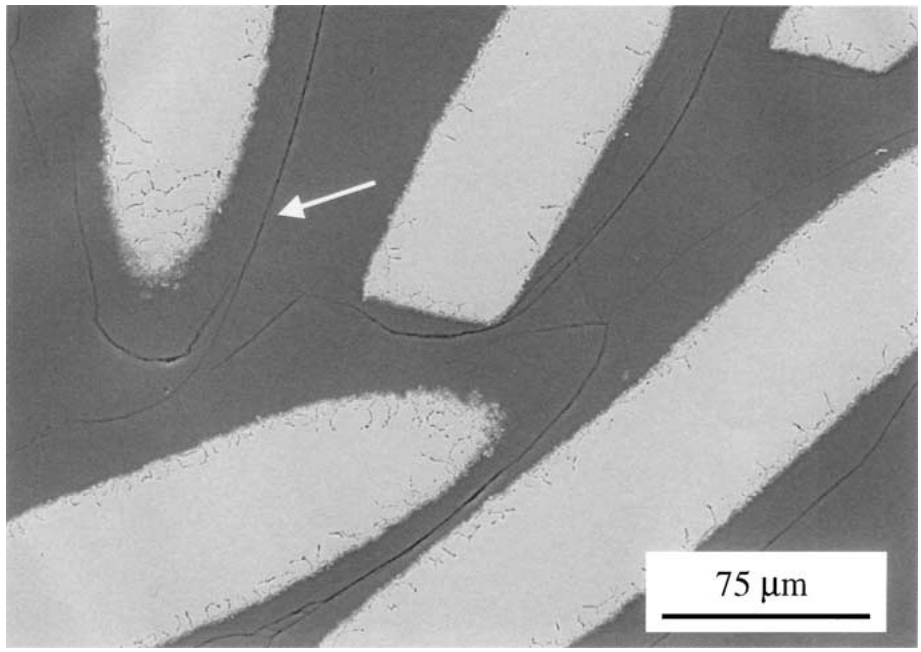

Figure 11 SEM micrograph showing a magnified area of Fig. 10, showing the circumferential cracks in the HA matrix but around the 316L fibres in the HA-25 vol% 316L fibre composite HIPed at 950 °C and 124 MPa.

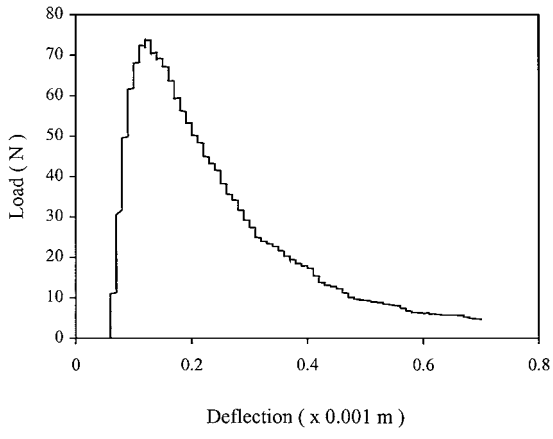

Figure 12 A curve of compression load versus deflection, showing the "pseudo-plasticity" of the HA-25 vol.% 316L composite.

bioactivity of the HA ceramics and the HA-316L fibre composites and the bio-inertness and surface roughness of the Si_3N_4 ceramics. The Si_3N_4 samples were significantly rougher than the HA and HA-fibre composite samples and, on the basis of Gross *et al*. [7], would be expected to have a much higher tensile strength if there were some compensatory chemical bonding mechanism(s). The absolute value of the interfacial tensile strength of the HA and HA-fibre composite samples is also high compared to literature values of 0.1 to 1.1 MPa [5, 7], especially at such an early time point.

It is noteworthy that, even at 4 weeks, the tensile strength of the newly formed bone (hole sample) was twice of that of the HA containing samples. This reflects the challenge in replacing natural bone with artificial materials. These data are from a very early time point in

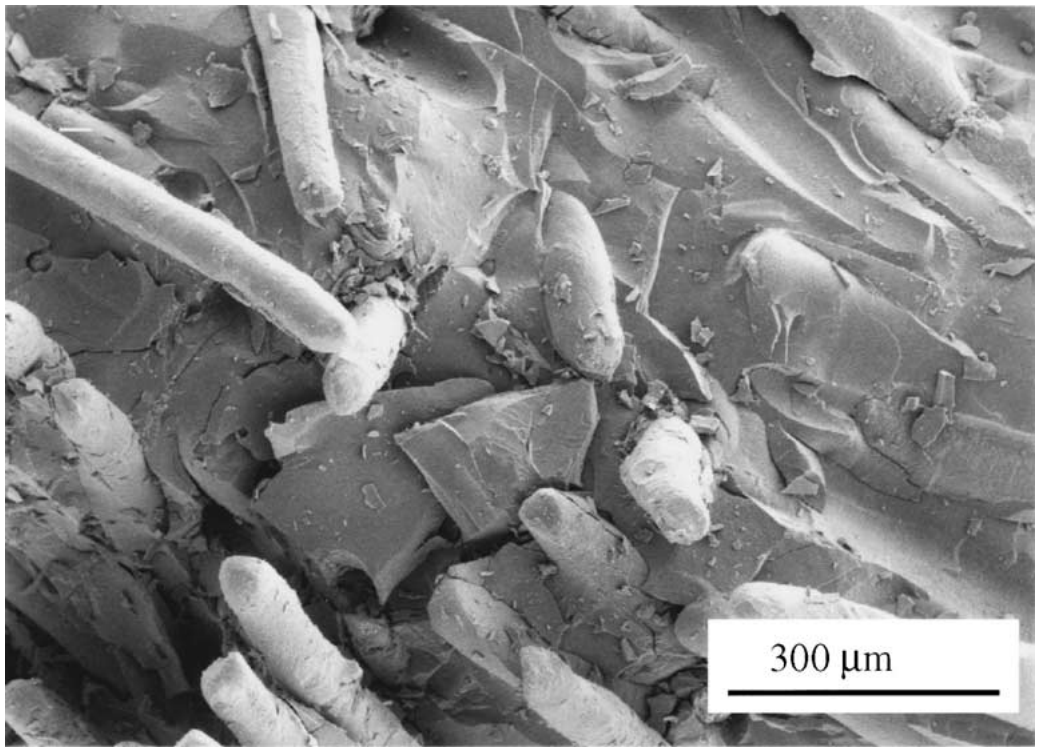

Figure 13 SEM micrograph showing the protruding fibres on the fracture surface.

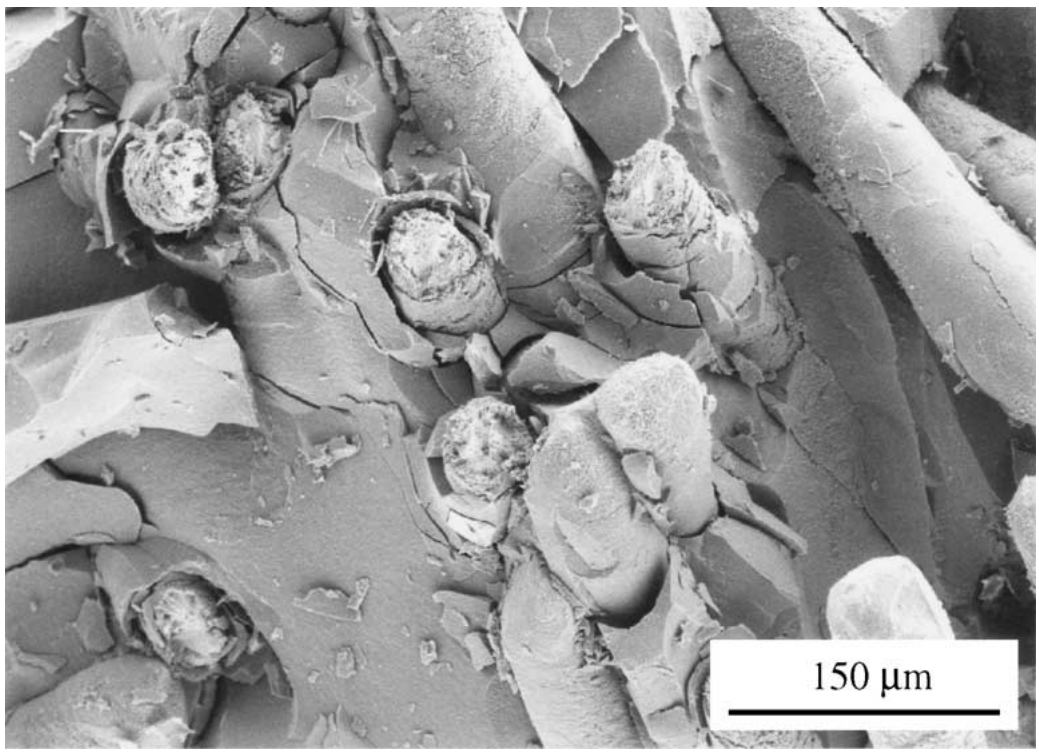

Figure 14 SEM micrograph showing the broken fibres on the fracture surface.

the bone repairing process and are a long way from the strength of the mature cortical bone (around 90 MPa) or long-term implantation as seen by Edwards *et al*. [5]. A comprehensive study involving much longer implantation time and detailed histological examination has been initiated.

4. Conclusions

The as supplied HA powder was porous and contained micron scale sized agglomerates of nanometre scale sized primary particles of low crystallinity, whereas the calcined HA powder was relatively dense agglomerates of submicron scale sized primary particles of high crystallinity. Compared with the as-supplied HA powder, the calcined HA powder resulted in much higher solids loading of the HA-316L slurries castable under vibration, which in turn led to much lower drying shrinkage of the cast bodies and much higher relative density of the green compacts.

Solids loading up to 44 vol% for the calcined HA powder derived mixtures were obtained at the Na-cmc addition level of around 0.5 wt% (solid basis). The

resultant relative density of the green compacts (cast and dried) was 46%. The relatively low solids loading and green density was traded off against the homogeneity of the 316L fibres dispersed in the HA matrix powder. Cold isostatic pressing of the green compacts increased the relative density of the green compacts from 46% after casting to 60% after CIPing.

In the preparation of the HA-316L fibre composites, some difficulties were encountered including the uniform distribution of the 316L fibres without segregation and clustering and the densification of the composites without decomposition of the HA component. However, uniform green compacts of the HA-316L fibre (up to 30 vol%) mixtures could be prepared by solid slip casting under vibration with the optimised thixotropic slurries that were able to prevent the dense and large 316L fibres from the preferential sedimentation. Vibration casting-cold isostatic pressing-hot isostatic pressing resulted in dense (99% theoretical density) and uniform HA-316L fibre composites without the decomposition of the HA component.

The HA-316L composites exhibited improved fracture toughness of 3.6 ± 0.3 MPa $\cdot$ m$^{0.5}$ compared with $\sim$1 MPa $\cdot$ m$^{0.5}$ of pure HA ceramics. The "pseudo-plasticity" of the composites may be due to the bridging of propagating cracks by the ductile 316L fibres. However, the mechanical strength of the composites was not improved due to the presence of the circumferential microcracks in the matrix. In addition, the early stage of biological assessment indicated that the composites were biocompatible and demonstrated advantageous bone-bonding performance compared to a bio-inert ceramic.

Acknowledgments

The authors wish to thank the Australian Research Council (ARC) for the provision of a research grant for the current project and the Australian Institute for Nuclear Science and Engineering (AINSE) for a grant-in-aid for the use of the cold and hot isostatic presses. The first author would also like to acknowledge Prof. C. C. Sorrell and Mr. D. Russell (University of New South Wales), and Dr. Dan Perera and Mr. S. Moricca (Australian Nuclear Science and Technology Organisation) for their cooperation and suggestions during the preparation of this paper.

References

1. F. B. BAGAMBISA, U. JOOS and W. SCHILLI, *J. Biomed. Mater. Res.* **27** (1993) 1047.
2. K. SOBALLE, E. S. HANSEN, B. H. RASMUSSEN and C. BUNGER, *J. Bone Joint Surg. (B)* (1993) 270.
3. M. J. COATHUP, P. BATES, P. COOL, P. S. WALKER, N. BLUMENTHAL, J. P. COBB and G. W. BLUNN, *Biomaterials* **20** (1999) 793.
4. G. WILLMANN, *British Ceramic Transactions* **95**(5) (1996) 212.
5. J. T. EDWARDS, J. B. BRUNSKI and H. W. HIGUCHI, *J. Biomed. Mater. Res.* **36** (1997) 454.
6. H. LIN, H. C. XU, X. D. ZHANG and K. DE GROOT, *ibid.* **43** (1998) 113.
7. U. GROSS, H.-J. SCHMITZ and V. STRUNZ, in "Biological and Biomechanical Behaviour of Biomaterials," edited by P. Christel, A Meunier and A. J. C. Lee (Elsevier Science, Amsterdam, 1988) p. 367.
8. W. SUCHANEK and M. YOSHIMURA, *J. Mater. Res.* **13**(1) (1998) 94.
9. G. ZIEGLER, in "Designing with Structural Ceramics," edited by R. W. Davidge and M. H. van de Voorde (Elsevier, London, 1991) p. 111.
10. R. ROGIER and F. PERNOT, *J. Mater. Sci.: Mater. In Med.* **2** (1991) 153.
11. G. DE WITH and A. J. CORBIJN, *J. Mater. Sci.* **24** (1989) 3411.
12. L. P. SIMOES, R. N. CORREIA and M. M. ALMEIDA, in "Bioceramics, vol. 4," edited by W. Bonfield, G. W. Hastings and K. E. Tanner (Butterworth-Heinemann Ltd, London, 1991) p. 91.
13. F. LELIEVRE, D. BERNACHE-ASSOLLANT and T. CHARTIER, *J. Mater. Sci.: Mater. In Med.* **7** (1996) 489.
14. A. J. RUYS and C. C. SORRELL, *Ceramic Bulletin* **69**(5) (1990) 828.
15. A. J. RUYS, S. A. SIMPSON and C. C. SORRELL, *J. Mater. Sci. Letts.* **13** (1994) 1323.
16. D. W. RICHERSON, "Modern Ceramic Engineering," 2nd ed. (Marcel Dekker, New York, 1992) p. 190.
17. I. SUSHUMNA, R. K. GUPTA and E. RUCKENSTEIN, *J. Mater. Res.* **6** (1991) 1082.
18. J. W. HALLORAN, in "Ultrastructure Processing of Ceramics, Glasses, and Composites," edited by L. L. Hench and D. R. Ulrich (John Wiley & Sons, New York, 1984) p. 404.
19. H. A. BARNES, *J. Non-Newtonian Fluid Mech.* **70** (1997) 1.
20. T. GARINO, *J. Dispersion Science and Technology* **18**(3) (1997) 273.

Received 20 October 1998
and accepted 26 December 2000